Heterojunction Resonant Tunneling Diode at the Atomic Limit

Ram Krishna Ghosh
Department of Electrical Engineering
The Pennsylvania State University
University Park, Pennsylvania, 16802, United States
e-mail: rug22@psu.edu

Joshua A. Robinson
Department of Materials Science and Engineering and
Center for 2-Dimensional and Layered Materials
The Pennsylvania State University
University Park, Pennsylvania, 16802, United States

Yu-Chuan Lin
Department of Materials Science and Engineering and
Center for 2-Dimensional and Layered Materials
The Pennsylvania State University
University Park, Pennsylvania, 16802, United States

Suman Datta
Department of Electrical Engineering
The Pennsylvania State University
University Park, Pennsylvania, 16802, United States line

***Abstract*—In this work, we present atomically thin resonant tunnel diode, based on vertically stacked heterostructures by combining graphene with layered transition-metal dichalocogenides (TMDs) such as molybdenum disulfide (MoS_2), and tungsten diselenide (WSe_2). Density functional theory (DFT) coupled with non-equilibrium Green's function (NEGF) transport calculation shows resonant tunnelling in heterolayer TMD and graphene (i.e. MoS_2-WSe_2-Gr) system with a prominent negative differential resistance (NDR) characteristic. However, homolayer TMD-graphene stack (i.e. bilayer WSe_2-Gr) does not show any NDR in its *I-V* characteristics.**

Keywords—heterostructure; tunneling; density functional theory; quantum transport

I. INTRODUCTION

Resonant tunnel diode is a subject of intense study, mostly in traditional semiconductor systems for many years due to its unique current transport phenomenon known as negative differential resistance (NDR). This negative differential conductivity holds the key for unique nanoelectronic design options utilizing bistability and positive feedback. Novel memories, multistate logic, oscillators and numerous other applications can benefit enormously from a low power, low voltage negative differential conductance device [1-2]. We can see an aggressive development on design optimization of resonant tunneling diodes (RTD), mostly in III-V heterostructure material systems, for many years now. However, unavoidable interface roughness scattering in conventional semiconducting materials makes it really challenging to obtain a prominent NDR at room temperature. In recent times, the absent of out of plane dangling bonding at the interface in multilayer stacking of two dimensional (2D) materials makes an interesting alternative to traditional semiconductors, and can improve the interfacial imperfections that limit room temperature NDR performance of the RTDs [3]. Currently, there are various combinations of graphene bas-

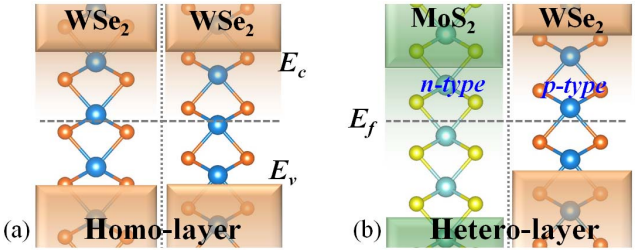

Fig. 1. Schematic showing band offset in (a) homo (bilayer WSe_2) and (b) heterolayer (MoS_2-WSe_2) TMDs. In the MoS_2-WSe_2 heterolayer system, n-type MoS_2 and p-type WSe_2 forms II type staggered heterojunction. E_c, E_v and E_f represent conduction band, valence band and Fermi energy, respectively.

ed 2D materials that are prominent to realize NDR in 2D heterostructure systems, however, combination of different transition metal dichalcogenides presently catch remarkable attention for their uniqueness when they form a heterojunction. Interestingly, semiconducting 2H-TMD materials normally have direct band gap in monolayer forms [4], however, when two different pristine TMD monolayers assemble to form a heterostructure then their interlayer van der Waals (vdW) interaction leads to new electronic properties. Especially, individual layers become *n* or *p*-type in nature and create a conduction or valence band offset. For example, in a MoS_2-WSe_2 heterolayer system, MoS_2 turns into *n*-type whereas WSe_2 becomes *p*-type and that forms a type II staggered gap heterojunction (Fig. 1) [5]. This unique nature in heterolayer TMD plays a key role to realize NDR in multilayer system. Very recently, Lin *et al.* [6] has experimentally demonstrated a spectrally narrow room temperature NDR in atomically thin synthetic stack of multijunction TMD-graphene systems. To understand the internal origin of this NDR in TMD materials, here, in this work we demonstrate an atomistic study on vertically stacked heterostructures by combining graphene with layered transition-metal dichalocogenides (TMDs) such as molybdenum disulfide (MoS_2), and tungsten diselenide (WSe_2).

978-1-4673-7860-4/15/$31.00 ©2015 IEEE

II. Computational Details

We perform non-equilibrium ballistic transport calculations by combining DFT with NEGF formalism to obtain the carrier transport in this vertical diode, where DFT uses the generalized gradient approximations (GGA) under Perdew-Burke-Ernzerhof (PBE) correlation function along with Grimme's DFT-D2 vDW corrections as implemented in Atomistic-ToolKit (ATK) [7].

The device configuration of our simulation is shown in Fig. 2. To construct the nano-device, we first utilize a supercell of MoS_2 /WSe_2 /4-layer Gr that is periodic in the x and y directions. To construct the interface we merge 3×3 supercell of mono-layer TMDs with 4×4 graphene to reduce the lattice mismatch between the di-chalcogenides and graphene hexagonal unit cell. The spin-orbit coupling is not considered here to reduce the computational complexity in our device simulations. We optimize the structure by using Quasi-Newton method until all the forces acting on atoms become smaller than 0.02 eV/Å. The structure optimization provides a van der Waals distance of 3.53 Å between WSe_2 and graphene and 3.41Å between MoS_2 and WSe_2. We place this optimized supercell on Pt (111) surface (applying the strain on Pt only) to modelled the electrode where we again do the structure optimization by keeping the lattice parameters fixed, so that the effect of extra strain due to Pt is restricted to the Pt(111) surface. This active region is then attached to two semi-infinite ideal electrodes where left is the Pt(111) electrode (extension of the Pt from the active region) and right is the graphene electrode (extension of 3 from Gr layers from the active region). For the self-consistent NEGF simulations, the Brillouin zone of the superlattice was sampled by 5×5 ×101 k-point grid along with a mesh cutoff energy of 150 Ry and with the same parameters as used before to calculate the electronic bandstructure. These numerical parameters are quite sufficient to attain a total energy convergence of 0.01 meV/unit cell within the self-consistent loop of the simulation of the device.

Under steady state transport, the NEGF formalism works with two principal quantities, the retarded Green's function $G^R(E)$, and the lesser Green's function $G^<(E)$. These define the accessible quantum states of the electrons and their occupancy into those states, respectively. In this formalism, the key quantity is to compute the Hamiltonian (H) and the overlap matrix (S) from the self-consistent DFT loop of the density matrix $\rho = (1/2\pi i)\int G^<(E)dE$.

Under local orbital basis set $\{\psi_i\}$, the Hamiltonian is defined as $H_{ij} = \langle \psi_i | \hat{H}_{KS} | \psi_j \rangle$ where $\hat{H}_{KS}$ is the Kohn-Sham Hamiltonian as obtained from the self-consistent DFT, whereas the overlap matrix is defined as $S_{ij} = \langle \psi_i | \psi_j \rangle$. From the knowledge of this H and S matrices along with the energy Eigen value matrix E of the system, one can construct the retarded Green's function, which is the only requisite for the calculation of coherent quantum transport [8]. Therefore, the retarded Green's function can be defined as

$$G^R_{k_\parallel} = [ES - H - \Sigma_{L,k_\parallel} - \Sigma_{R,k_\parallel}]^{-1} \quad (1)$$

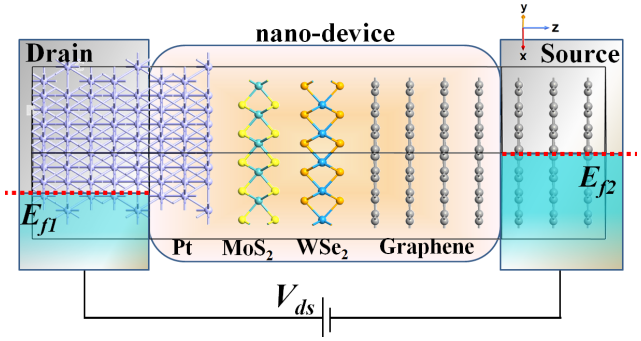

Fig. 2. (a) Schematic of the vertical nano-device setup of both of MoS_2-WSe_2-Gr and bilayer WSe_2 -Gr system used for quantum transport calculation. E_{f1} and E_{f2} indicate the corresponding Fermi levels of the left and right electrodes, respectively, for an applied positive bias V_{ds}.

where $\Sigma_{L,k_\parallel}$ and $\Sigma_{R,k_\parallel}$ are the self-energy matrices of the left and right electrode contacts, respectively. Using this, the transmission function can be easily given by

$$T(E,V,k_\parallel) = trace[\Gamma_{R,k_\parallel}(E)G^R_{k_\parallel}(E)\Gamma_{L,k_\parallel}(E)(G^R_{k_\parallel}(E))^\dagger] \quad (2)$$

in which $\Gamma_{L,k_\parallel}$ and $\Gamma_{R,k_\parallel}$ are the level broadening matrices $\left[\Gamma_{L/R,k_\parallel}(E) = (i/2)\{\Sigma_{L/R,k_\parallel}(E) - \Sigma^\dagger_{L/R,k_\parallel}\}\right]$ associated with the left and right electrodes, respectively, which are the anti-Hermitian components of the self-energies of the semi-infinite ideal electrodes. It can be then easily computed the current from left to right electrode as

$$I(V_{ds}) = \frac{2q}{h}\int_{BZ} dk_\parallel \int dE T(E,k_\parallel,V_{ds})\left[f\left(\frac{E-E_{f_1}}{k_BT}\right) - f\left(\frac{E-E_{f_2}}{k_BT}\right)\right] \quad (3)$$

where we assume the electrodes are infinite reservoirs characterized by the Fermi function $f(E-E_f)$ and the difference between the chemical potentials $E_{f_1} - E_{f_2} = qV_{ds}$ defines the applied bias for the self-consistent non-equilibrium transport. Here we want to note that, in our device simulations we use the applied bias at the left electrode (i.e. $E_{f_1} = E_f + qV_{ds}$) by keeping the right electrode bias at zero (i.e. $E_{f2} = E_f$) where the Fermi energy of the system is set to be zero in our NEGF calculation. Finally, the total current is expressed as the sum of both of the spin up and spins down components of the current. Further, to calculate the local density of states (LDOS) we use the formulation,

$$D(E,r) = \sum_{i,j} \rho_{i,j}(E)\psi_i(r)\psi_j(r) \quad (4)$$

where $\rho(E)$ is the spectral density matrix.

III. Result and Discussions

Within the NEGF+DFT framework for transport, the Hamiltonian of the system is solved by calculating the electronic charge distribution via the self-consistent DFT loop of the full density matrix of the device whose diagonal element describes the charge density. This procedure produces the bias-

dependent transmission function, $T(E, V, k_{||})$. We then extract the *I-V* characteristics from this transmission function as a function of applied bias in the ballistic transport regime which shows a pronounced NDR in both positive and negative bias regimes of the MoS_2-WSe_2-Gr heterostructure device (Fig. 3). During the calculation of the ballistic quantum transport, we see that the current exhibits a "soft" turn-on around a threshold voltage of ~0.4 V, increases to its peak value at $V = V_{peak}$~1.0 V, and then decreases as the bias voltage is increased, with an eventual "hard" turn on at 1.2 V within the positive bias regime. This feature can easily be explained by the bias dependent transmission spectra as shown in Fig. 4. Within the Fermi window of 0-0.4 eV, we can see that the carrier transmission is effectively negligible due the absence of any transmission channel. Above 0.4 eV, the transmission becomes finite and the current starts increasing with the applied bias, where the primary transmission resonance peaks (peak P1, P2 and P3 in Fig. 4) appear at approximately 1.0 V and then get suppressed with further increase in applied bias. It is this peak and valley in the transmission spectra arising from resonant tunneling phenomenon that leads to the observed NDR. When the bias is further increased, conventional tunneling occurs due to the high density of states (DOS) at higher energy levels, and the current increases exponentially thereafter. Very recently, this NDR characteristics has been discovered experimentally in TMD based van der Waals heterostructures [6], [9].

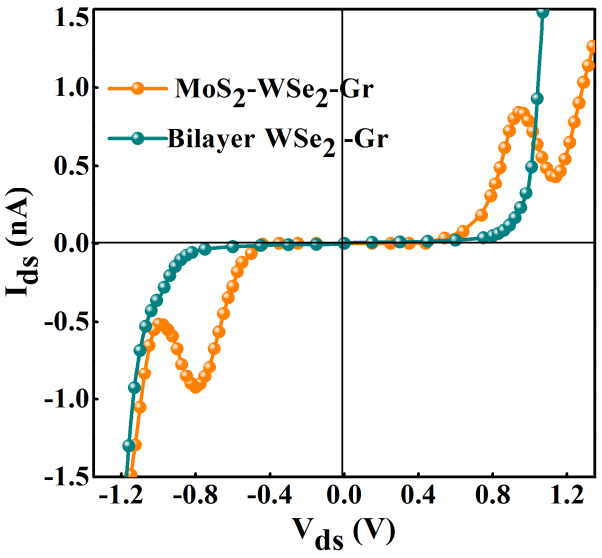

Fig. 3. Simulated *I-V* curves of the vertical tunnel junctions for both the hetero and homostructure.

The transmission Eigen states at the energetic location of the three strong peaks for a bias of +1.0V (Fig 4) provides clue to the microscopic origin of the NDR in the MoS_2-WSe_2-Gr heterostructure. Inspection of the localized molecular orbitals of the Eigen states in Fig. 5 reveals that all three resonance peaks originate from a combination of the Pt (*s*-orbital), WSe_2 (*p*-orbital of Se, W and *d*-orbital of W) and different graphene layers (*p*-orbital). Interestingly, in the case of MoS_2-WSe_2-Gr heterostructure, the MoS_2 in direct contact with the Pt electrode, and the first graphene layer closest to the WSe_2 TMD do not contribute to the strong transmission peaks, instead they

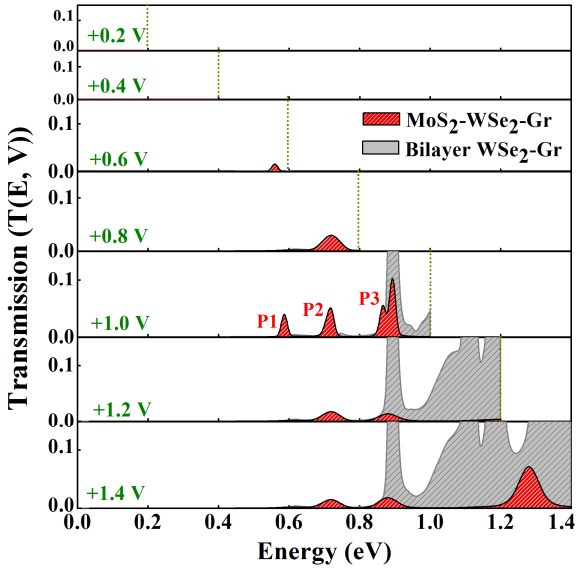

Fig. 4. Energy and bias dependent transmission as self-consistantly calculated for each applied positive bias voltage. The dotted line indicates the Fermi window for that applied bias voltage accross the terminals.

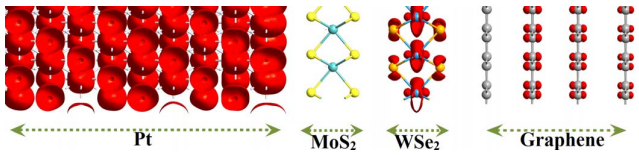

Fig. 5. Transmission Eigen states that contribute to the transmission in the peak P3 of the transmission at an applied bias V = +1.0V in the MoS_2-WSe_2-Gr heterostructure. Similar contribution of Eigen states has been observed in other two peaks also.

act as tunnel barriers. Further, the interatomic electronic interaction between the 2D layers makes MoS_2 *n*-type and WSe_2 *p*-type, which indicates that the transmission Eigen states in the resonant peaks originate from the WSe_2 hole energy states confined by the MoS_2 and the Gr tunnel barrier layers.

In theory, the necessary condition for resonant tunneling is based on alignment of energy levels in the contacts and the confined 2D layer (WSe_2 layer in this positive bias case) as well as the conservation of the transverse momenta [10]. Therefore, we study the position-dependent local density of states (LDOS), ($N(z, E)$, eq. 4) between the Pt and graphene electrodes at the peak voltage of +1.0 V (Fig. 6). We know that, with the application of positive bias, the Fermi level in the *Pt* electrode is lowered with respect to the graphene electrode Fermi level as shown in Fig. 2. If we identify the energetic locations of the corresponding transmission peaks in Fig. 4 and map with the energy positions in the local density of states (LDOS) in Fig. 6 we find that the hole energy states in the WSe_2 layer contribute to the transmissions. The strong coupling between the available states from the Pt electrons (or holes) with the WSe_2 holes and the graphene holes provides resonant conduction states enclosed by the chemical potential of the Pt and the graphene electrodes. Therefore, we conclude that the orbital contribution to the transmission Eigen states of

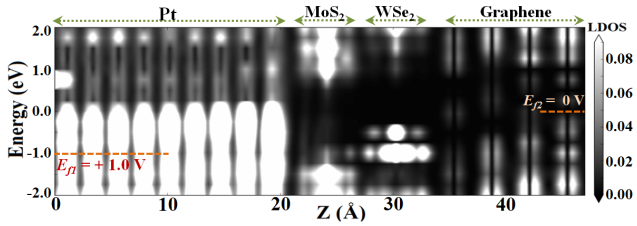

Fig. 6. Local density of states (LDOS) of MoS_2-WSe_2-Gr heterostructure at V_{ds} = +1.0 V of the nano-device.

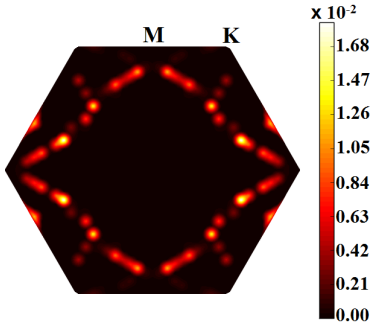

Fig. 7. ***k***-resolved transmission of the peak P3 in the T(E,V) plot with the hexagonal Brillouin zone provides insight into the physical origin of the resonant tunneling.

the resonant peaks are due to the confinement of holes in WSe_2 by the MoS_2 arising from valence band offset for the applied positive bias condition. The LDOS plot further points out that interatomic electronic interaction between MoS_2 and WSe_2 makes them *n*- and *p*-type, respectively; which is in good agreement with other theoretical work [5]. We also confirmed the conservation of the transverse wave vector-*k* during the resonant tunneling process. The *k*-resolved spectra of the three resonant transmission peaks within the hexagonal Brillouin zone (BZ) (Fig. 7) of the MoS_2-WSe_2-Gr Van der Waals heterostructure arise from "sharp" spikes at specific points in the Brillouin zone. This phenomenon corresponds to resonant tunneling due to the conservation of the momentum during this resonant tunneling process. In contrast, conventional tunneling would result in a diffuse transmission spectrum over the entire Brillouin zone [11]. Therefore, in positive bias regime, WSe_2 effectively acts as a quantum well confined by the MoS_2 barrier in this vertical tunnel diode. Conversely, with the application of negative bias, the Fermi level in the *Pt* electrode will elevate with respect to the graphene electrode Fermi level and the confined electrons in MoS_2 due to this conduction band offset offers the necessary bound states of the resonant tunneling in the negative bias regime to obtain the NDR. On the other hand, bilayer WSe_2 does not offer any band offset in the energy band diagram and its bandgap acts as a regular electronic barrier in the carrier tunneling. Our calculated transmission in bilayer WSe_2 -Gr system (Fig. 4) clearly reflects this nature and shows no NDR in its *I-V* characteristics (see Fig. 3).

IV. Conclusions

We have demonstrated the quantum transport mechanism in two different TMD-Gr multilayer structures through DFT coupled with NEGF transport calculation. The energy band offset in heterolayer TMD controls the resonant tunnelling to produce NDR feature the in MoS_2-WSe_2-Gr devices whereas the enegy bandgap of homolayer TMD in bilayer Wse2 -Gr system acts like a regular diode.

Acknowledgment

This work was supported by the Center for Low Energy Systems Technology (LEAST), one of six centers supported by the STARnet phase of the Focus Center Research Program (FCRP), a Semiconductor Research Corporation program sponsored by MARCO and DARPA.

References

[1] H. L. Chan, S. Mohan, P. Mazumder, and G. I. Haddad, "Compact multiple-valued multiplexers using negative differential resistance devices," IEEE J. Solid-State Circuits, vol. 31, pp. 1151–1156, Aug. 1996.

[2] V. V. Mitin, V. Kochelap, and M. A. Stroscio, "Quantum Heterostructures: Microelectronics and Optoelectronics," Cambridge Univ. Press, 1999.

[3] L. Britnell, R.V. Gorbachev, A.K. Geim, L.A. Ponomarenko, A. Mishchenko, M.T. Greenaway, T.M. Fromhold, K.S. Novoselov, and L. Eaves, "Resonant tunnelling and negative differential conductance in graphene transistors," Nat. Commun., vol. 4, pp. 1794(1)–(5), Apr. 2013.

[4] R. K. Ghosh, and S. Mahapatra, "Monolayer Transition Metal Dichalcogenide Channel-Based Tunnel Transistor," IEEE J. Electron Devices Soc. Vol. 1, pp. 175–180, Nov. 2013.

[5] C.-H Lee, G.-H. Lee, A. M. van der Zande, W. Chen, Y. Li, M. Han, X. Cui, G. Arefe, C. Nuckolls, T. F. Heinz, J. Guo, J. Hone, and P. Kim, "Atomically thin p–n junctions with van der Waals heterointerfaces," Nat. Nanotechnol. vol. 9, pp. 676–681, Aug. 2014.

[6] Y.-C. Lin, R. K. Ghosh, R. Addou, N. Lu, S. M. Eichfeld, H. Zhu, M.-Y. Li, X. Peng, M. J. Kim, L.-J. Li, R. M. Wallace, S. Datta, and J. A. Robinson, "Atomically thin resonant tunnel diodes built from synthetic van der Waals heterostructures," Nat. Commun, vol. 6, pp. 7311(1)–(6), Jun. 2015.

[7] QuantumWise simulator, Atomistix ToolKit (ATK). Online at <www.quantumwise.com>

[8] S. Datta, "Quantum Transport-Atom to transistor," Cambridge Univ. Press, 2005.

[9] T. Roy, M. Tosun, X. Cao, H. Fang, D.-H Lien, P. Zhao, Y.-Z. Chen, Y.-L. Chueh, J. Guo, and A. Javey, "Dual-Gated MoS_2/WSe_2 van der Waals Tunnel Diodes and Transistors," ACS Nano vol. 9, pp. 2071–2079, Jan. 2015.

[10] S. M. Sze and K. K. Ng, "Physics of Semiconductor Devices," 3rd ed. Hoboken, NJ, USA: Wiley, 2007.

[11] J. M. MacLaren, X.-G. Zhang, and W. H. Butler, "Validity of the Julliere model of spin-dependent tunneling," Phys. Rev. B, vol. 56, pp. 11827-11832, Mar. 1997.